Energy and Buildings 151 (2017) 146–156

Contents lists available at ScienceDirect

Energy and Buildings

journal homepage: www.elsevier.com/locate/enbuild

On the analytical calculation of the solar heat gain coefficient of a BIPV module

T. Baenas [a,*], M. Machado [b]

[a] Department of Applied Mathematics, University of Alicante, Ctra. de S. Vicente del Raspeig s/n, 03690 S. Vicente del Raspeig, Alicante, Spain
[b] Energy and Environment Division, Tecnalia Research and Innovation, Paseo Mikeletegi, 2, 20009 San Sebastián, Guipúzcoa, Spain

ARTICLE INFO

Article history:
Received 20 March 2017
Received in revised form 19 May 2017
Accepted 16 June 2017
Available online 23 June 2017

Keywords:
Thermal performance
Semitransparent BIPV
Solar heat gain coefficient
Glazing systems
Solar factor

ABSTRACT

A closed-analytical expression for the solar heat gain coefficient (SHGC) of a glass-glass photovoltaic module for building-integration is constructed *ab initio*, from the thermal study of the general case of any number of planar parallel layers with homogeneous absorption of solar radiation. By introducing the optical model of Baenas and Machado, the expressions for the SHGC of the opaque and transparent parts of the module will be provided. The scope of the calculation and the assumed working hypothesis are in line with those of international standards for multiple glazing systems and building-integrated photovoltaic modules. The proposed model has been applied to a real case of study, showing an excellent agreement with the numerical and experimental related data.

1. Introduction

Building-integrated photovoltaic (BIPV) market has experienced a considerable expansion in the past decades and a continuous development is expected for the following years. One of the main drivers for BIPV market growth is the increasingly demanding legislation related to energy performance in buildings. The building sector, responsible for 40% of the total energy consumption in the EU,[1] provides a largely untapped and cost-effective potential for energy savings. Energy related directives, building codes and standards are therefore amongst the most important measures for energy efficiency in buildings. In the EU, for example, the Energy Performance of Buildings Directive [1] 2010/31/EU and the Energy Efficiency Directive [2] 2012/27/EU constitute the main legislation in relation to energy consumption reduction in buildings. Within this framework, the introduction of passive energy saving strategies is key, but also renewable energy technologies, and in particular the integration of photovoltaic (PV) systems in the building envelope, offer many possibilities to play a key role within the Nearly Zero Energy Buildings scenario.

The use of semitransparent glazed BIPV products in skylights and façades is rapidly increasing, offering a good balance between aesthetics, efficiency, cost and multifunctionality in the building environment. Glass-glass PV laminates may be combined with additional glass panes in double or triple glazing systems and also with added coatings or colored elements to provide improved aesthetics, shading during the summer, natural lighting and thermal insulation during the winter, acoustic insulation and mechanical safety, among other functionalities.

This growing implementation of semitransparent BIPV elements and the need to comply with energy performance related legislation and national building codes implies for architects, thermal engineers and manufacturers the need to have access to the thermal transmittance coefficient (*U*-value) and solar heat gain coefficient (SHGC) values, which are typically used for comparison between glazing systems and as inputs for building energy performance simulations.

The SHGC, also named as *g*-value or solar factor, is the total solar energy transmittance factor through a glazing system separating two environments (generally outdoor and indoor). A standardized definition of this magnitude in the case of transparent glazing systems is given by, mainly, ISO 9050 [3] or EN 410 [4] for a simplified calculation, *i.e.*, avoiding the resolution of the non-linear system of equations for the heat balance. A detailed calculation in which conductive-convective and radiative parts of the heat transport problem are coupled through the temperature nodes, is provided by ISO 15099 [5] and EN 13363-2 [6]. The latter standards follow a

* Corresponding author.
E-mail addresses: tomas.baenas@ua.es (T. Baenas), maider.machado@tecnalia.com (M. Machado).

[1] See, *e.g.*, the proposal for the amendment of Directive 2010/31/EU on the energy performance of buildings (2016), http://ec.europa.eu/energy/en/topics/energy-efficiency/buildings.

http://dx.doi.org/10.1016/j.enbuild.2017.06.039

Nomenclature

A	spectral absorptance
$\bar{A}$	solar-spectrum integrated absorptance
$\bar{A}_i$	ith layer solar-spectrum integrated absorptance
e_i	ith layer thickness, [m]
g	SHGC (solar heat gain coefficient)
f	ratio of transparent to total area
h	combined heat transfer coefficient, [W/(m^{2}K)]
h^{conv}	convective heat transfer coefficient, [W/(m^{2}K)]
h^{rad}	radiative heat transfer coefficient, [W/(m^{2}K)]
I	solar irradiance, [W/m^2]
k_i	ith layer thermal conductivity, [W/mK]
P_{el}	electrical (DC) PV generation power, [W/m^2]
q	steady-state heat flux without solar irradiance, [W/m^2]
q^s	steady-state heat flux with solar irradiance, [W/m^2]
$q_{i,i+1}$	steady-state heat flux between ith and $(i+1)$th nodal planes, [W/m^2]
r_i	i component interface spectral reflectivity
R_i	ith layer thermal resistance, [m^{2}K/W]
R_{tot}	total thermal resistance of the system, [m^{2}K/W]
R	spectral reflectance
$\bar{R}$	solar-spectrum integrated reflectance
$\tilde{R}_{i,i+1}$	modified thermal resistance between ith and $(i+1)$th layers, [m^{2}K/W]
S	normalized relative spectral distribution of the solar radiation, [m^{-1}]
T_i	ith node temperature without solar irradiance, [K]
T_i^s	ith node temperature with solar irradiance, [K]
T_m	temperature mean value, [K]
T	spectral transmittance
$\bar{T}$	solar-spectrum integrated transmittance
U	U-value (thermal transmittance coefficient), [W/(m^{2}K)]
β_e	Hermanns et al.'s parameter (direct absorptance moment)
β_{ref}	linear temperature coefficient (at reference temperature), [K^{-1}]
γ	Rosenfeld's parameter (normalized average thermal resistance)
ε	hemispherical emissivity
δq	steady-state heat flux difference between solar irradiance and no solar irradiance cases, [W/m^2]
η	PV cell conversion efficiency
ϕ	spectral solar flux factor
$\bar{\phi}$	solar-spectrum integrated flux factor
λ	wavelength, [m]
τ_i	i component substrate spectral transmissivity
σ	Stefan-Boltzmann constant, [W/(m^{2}K)^4]
θ	irradiation angle of incidence, [rad]
θ_r	irradiation angle of refraction, [rad]

Special subscripts and superscripts

bare	bare PV cell (not encapsulated)
cal	analytically calculated value
cell	PV cell
eff	effective (absorptance)
ec	encapsulated PV cell
enc	encapsulation materials (glass and polymers)
exp	experimental value
f/*b*	front/back directions
gi	ith glass layer
in/*out*	boundary indoor (or incoming)/outdoor (or outcoming)
l	polymer interlayer
num	numerically calculated value
ref	reference conditions

different approach, by considering either a node of temperature in each glass surface, or a sole node for each layer, respectively.

Therefore, for glazing systems with no PV cells embedded, different mathematical procedures for the calculation of the SHGC and thermal transmittance are included in the previously mentioned standards: in the case of the simplified calculation, closed-analytical expressions are provided, while iterative procedures must be applied for a detailed calculation. Concerning the normative framework of BIPV, the recently published EN 50583 [7] standard, parts 1 and 2, for BIPV modules and systems states the need to determine U- and g-values for BIPV systems, but no specific calculation procedure is provided, beyond references to the glazing standards. For the determination of the solar factor of semi-transparent BIPV glass–glass modules, the analysis of heat transfer through the system should consider both the surface covered by opaque PV cells (opaque region) and the transparent glazed part (transparent region). In this sense, the detailed thermal and optical modelling of the area occupied by the cells is missing in currently available standards.

In this paper, an analytical determination of the SHGC of a glass-glass photovoltaic module for building-integration is provided, starting from the thermal study of a general system of any number of planar parallel layers with homogeneous absorption of solar radiation (short-wave spectrum), and opaque to infrared radiation. An accurate description of the optical performance is included through the application of the optical model of Baenas and Machado [8] and Machado et al. [9]. The scope of this analytical model and its assumed working hypothesis are in line with those of international standards for multiple glazing systems. However, it improves the accuracy of the optical and thermal modeling, with respect to the standardized simplified calculation, and it completes the description of the opaque region by introducing the effective short-wave absorptance of the solar cell. This effective absorptance takes into account the ability of the solar cell to convert a portion of the solar irradiation into electrical energy.

The features of the model presented herein allow the achievement of results with the same accuracy levels as those of the iterative procedures, under standardized boundary conditions. This is accomplished through closed-analytical expressions and a set of physical parameters that can be quantified by following the procedures from the related standards – including the experimental optical characterization of the encapsulation materials – or even from the technical data provided by the manufacturers for the different components, leading to a determination of the SHGC from design parameters. However, this operational advantage is related with the standardized-like set of environmental conditions used in the simplified calculation, which is very useful for BIPV applications. Obviously, it cannot hold for any set of boundary conditions, as the non-linear equations and coupling effects within the heat transfer problem cannot be avoided in general, due to the involved physical laws.

Several studies can be found in the specific literature on the thermal performance of semitransparent BIPV modules using numerical procedures, with different modelling approaches. For instance, Fung and Yang [10] provided a rigorous calculation of the so-called semi-transparent photovoltaic module heat gain (SPVHG), which is equivalent to the g-value, by numerically solving

a one-dimensional transient heat transfer model of a glass-glass PV module. Further interesting numerical studies on the thermal performance of BIPV systems can be found, among others, in Skandalos and Karamanis [11], Vats and Tiwari [12], Infield et al. [13,14], Wong et al. [15], Wang et al. [16], Han et al. [17], Chow et al. [18] or Liao [19] and Guardo et al. [20] (the last two ones using two-dimensional computational fluid dynamics – CFD – to model the heat transfer phenomena). A recent compilation of different modelling approaches for the thermal analysis of BIPV systems has been performed as a result of the SOPHIA Photovoltaic European Research Infrastructure FP7 project.[2]

These numerical studies contextualize the importance and the need to obtain estimations for the *g*-value from the design phase of BIPV modules, though this issue is approached from a complementary perspective to the one followed in this work. They provide a clear view on the general design parameters used for the theoretical study of the thermal performance, the accuracy of numerical predictions and the simplifications of the modelling, some of which (in particular, those regarding the optical performance) can be improved, as will be shown herein.

In a similar way, Mazzali et al. [21] used a finite difference model to solve the heat transport problem. This work will be further analyzed in Section 4, as it includes a direct experimental measurement of the SHGC in standardized boundary conditions which will be used herein to test the results of the theoretical model presented. Note that the experimental characterization of the SHGC is a costly and complex matter (see, *e.g.*, in the scope of BIPV, Chen et al. [22], Pahud et al. [23], Olivieri et al. [24], Kuhn [25] and the previously mentioned Mazzali et al. [21]).

The experimental measurement of the solar factor is not a requirement from BIPV or glass for building standards, and it is not a service usually offered by research centers, laboratories of notified bodies, though available in some of them. Experimental characterization, based on the use of calorimeters, is costly and onerous for the usual industry needs.

None of the previous works includes an optical characterization of the absorptance of the solar cell, through the layer-by-layer calculation of the short-wave energy fluxes (ISO 15099, [5], or Baenas and Machado [8] and references therein). This key physical parameter is included in the formerly mentioned thermal models either as a design parameter or by numerically fitting through an experimental calibration. Although these calculation procedures are technically valid within the different purposes of each study (for instance, an accurate evaluation of the annual total heat gain of the PV system), the common and practical use of the *g*-value, mainly by the glazing and façade industries, requires a complete *a priori* calculation of the SHGC, in line with the recent requirements of EN 50583 [7] standard. There is a need in these sectors to determine in advance the optical and thermal properties of the glazing elements, under the different and multiple configurations that can be considered in the design phase of the building envelope. An example of an application of this type is shown in Machado et al. [9], where optical analytical modeling is used to predict PV cell efficiencies with different encapsulation materials (mainly glass and polymers).

In this sense, Moralejo et al. [26] performed the optical characterization of a set of BIPV modules through the ISO 9050 [3]/EN 410 [4] standards, and used the simplified standardized expression for the *g*-value. This is also the approach taken in, *e.g.*, Misara's [27] or Shen's [28] dissertations, in order to tackle with the thermal performance of BIPV modules.

In view of the above, the procedure developed herein incorporates a theoretical modeling of the optical and thermal performance of a BIPV system. The optical model requires the spectrophotometric characterization of a minimum number of configurations in order to obtain the spectral reflectivity of the encapsulation-cell interfase, after which the optical performance of other module configurations can be obtained from calculations [9]. The thermal modeling allows the calculation of the solar factor from standardized and/or design parameters (*e.g.*, experimentally characterized by the manufacturer). This calculation is performed here from a simplified approach, in line with EN 410 [4] and ISO 9050 [3] standards to which BIPV standard EN 50583 [7] refers, avoiding the non-linear calculation of the thermal balance equations. However, a detailed numerical calculation can be tackled from standardized procedures (ISO 15099, [5] and EN 13363-2, [6]) or the referenced literature on numerical studies. As a result, the presented method involves lower economic and execution costs than a fully experimental *g*-value determination.

This paper is structured as follows. In Section 2, the applied thermal model and the general definition of the SHGC for a multilayered system are developed *ab initio*. In Section 3, the proposed expression for the simplified calculation of the *g*-value and its main features are presented. This comprises the optical performance of the PV module, the modeling of the effective absorptance of the encapsulated solar cell, and their integration within the previous thermal model. In Section 4, an experimental and numerical comparison with external data will be provided, highlighting the operational advantages of the proposed procedure. Finally, some conclusions about the presented research will be drawn.

2. Thermal model fundamentals

2.1. Central nodal-plane approach

The theoretical basis of a one-dimensional short-wave absorption and thermal conduction problem, in steady-state, for a multilayered planar parallel glazing structure is revisited in this work. For the established purposes, an in accordance with current European and international regulatory framework, homogeneous and non-scattering media will be considered, within the hypothesis of uniform absorption of solar radiation, which represents very closely the real behaviour of glazing systems. For a comprehensive study of a more general situation – including non-uniform absorption – Rosenfeld [29] or Hermanns et al. [30], can be consulted (both models being indeed equivalent). The central nodal-plane approach, based on the equivalence of the uniform absorption hypothesis and the assumption that the short-wave absorption occurs in a nodal-plane in the center of the glass pane, is followed herein. This approach will simplify the handling of the thermal balance equations.

The incoming normal solar radiation flux (irradiance) will be henceforth denoted by I. A glass pane with thickness e and thermal conductivity k will be considered. Let $0 \leq \bar{A} \leq 1$ be the (standardized) solar-spectrum integrated absorption coefficient, $\bar{A}I$ being the absorbed radiation flux. Let T_1 and T_2 be the surface temperatures, and q_{in} and q_{out} the incoming and outcoming steady-state heat fluxes, respectively. All heat fluxes are defined per unit area. Let x be the transversal coordinate, positive as depicted in Fig. 1.

The uniform absorption hypothesis is mathematically established by means of the differential relation $dq = (\bar{A}I/e)dx$. This equation, together with the one-dimensional Fourier law (for steady thermal conduction), $q(x) = -kdT/dx$, leads to the well-known parabolic temperature profile inside the layer[3] after a

[2] Grant Agreement 262533, http://www.sophia-ri.eu/

[3] Within the glazing standards scope, see, *e.g.*, Eq. (32) of ISO 15099 [5].

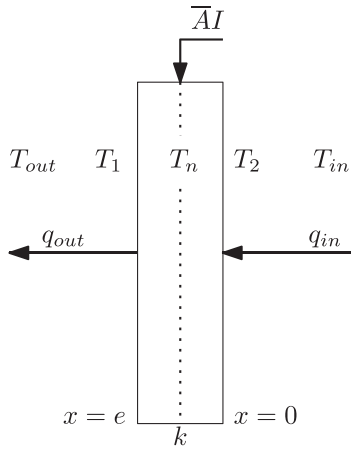

Fig. 1. Scheme of a layer with central nodal-plane.

double integration with the boundary conditions of the inner surface, $q(x=0)=q_{in}$ and $T(x=0)=T_2$,

$$q(x) = q_{in} + \frac{\bar{A}I}{e}x, \quad \frac{\bar{A}I}{e}x^2 + q_{in}x = -k[T(x) - T_2] \tag{1}$$

Therefore, by imposing the remaining boundary conditions of the outer surface, $q(x=e)=q_{out}$ and $T(x=e)=T_1$, the following relations are obtained,

$$\begin{aligned} q_{out} &= q_{in} + \bar{A}I, \\ \frac{\bar{A}I}{2} + q_{in} &= -\frac{T_1 - T_2}{R}, \end{aligned} \tag{2}$$

$R=e/k$ being the thermal resistance of the layer.

These algebraic expressions govern the steady-state thermal balance so that the heat fluxes q_{in} and q_{out} can be obtained from the constants of the problem. Eqs. (2) imply that it is not necessary to determine the temperature profile inside the media in order to obtain the boundary heat fluxes, which is the basis for the heat balance calculation with thermal resistances.

The central nodal-plane approach is a symbolic procedure to obtain Eq. (2), avoiding the integration process, by considering a central plane with temperature T_n where the absorption of the whole solar radiation takes place (see Fig. 1). This plane divides the glass pane into two parts, each of them accounting for half of the thermal resistance. So it can be considered that

$$q_{in} = -\frac{T_n - T_2}{R/2}, \quad q_{out} = -\frac{T_1 - T_n}{R/2}, \tag{3}$$

which can be added to the *ad hoc* assumption of $q_{out} = q_{in} + \bar{A}I$ to obtain

$$q_{in} + q_{out} = 2q_{in} + \bar{A}I = -\frac{T_1 - T_2}{R/2}, \tag{4}$$

or equivalently, Eq. (2). Note that the sign criterium selected for the heat fluxes is such that $q>0$ implies heat transfer from right (indoor) to left (outdoor).

2.2. Definition of the solar heat gain coefficient

As defined above, the SHGC or g-value, $0 \le g \le 1$, is the total solar energy transmittance of a glazing system (or fenestration element) separating two environments. It can be operatively defined by considering the steady-state heat fluxes in a twofold situation, when the system is exposed to solar irradiance from outdoor, q^s, or when there is no irradiance, q. Then, the SHGC is a dimensionless factor such that the following relation is fulfilled,

$$q^s = q - gI. \tag{5}$$

Then, the physical problem consists in obtaining the two contributions of the thermal gain of the system, *i.e.*, the one due to the direct transmission of the solar radiation flux, $\bar{T}I$, $\bar{T}$ being the (standardized) solar-spectrum integrated transmittance of the glazing, and the one due to the absorption-conduction problem, $|\delta q_{in}|$ (here the δ symbol stands for the heat flux difference with respect to the case of no solar irradiance), so that,

$$gI = \bar{T}I + |\delta q_{in}|. \tag{6}$$

In order to perform a simplified calculation, outdoor and indoor environments will be described by the thermal resistances between them and the system's inner and outer surfaces, $R_{out} = h_{out}^{-1}$, $R_{out} = h_{in}^{-1}$, h_{out} and h_{in} being the external and internal combined heat transfer coefficients. These are modelled through the convective and radiative parts of the thermal exchange between the system and the environment, $h_{in/out} = h_{in/out}^{conv} + h_{in/out}^{rad}$, under specific boundary conditions. Classical approximations exist (see, *e.g.*, Aguilar [31]) which allow a linear treatment of the combined convection–radiation heat transfer problem. For instance, by considering $T_{in} \simeq T_2$ and Stefan-Boltzmann law, the h_{in}^{rad} coefficient can be expressed as (with the notation from Fig. 1),

$$h_{in}^{rad} = \varepsilon\sigma\frac{T_{in}^4 - T_2^4}{T_{in} - T_2} \simeq 4\varepsilon\sigma T_m^3, \tag{7}$$

σ being the Stefan-Boltzmann constant, ε the hemispherical emissivity [32] and T_m the mean value of T_{in} and T_2, considered as a constant in a simplified calculation[4] (obviously, an analogous relation stands for the outdoor variables). It should be noted that Eq. (7) is an example of the Newton law of cooling, due to $q_{in} = h_{in}(T_{in} - T_2)$ with h_{in} being (approximately) constant.

For the standardized simplified approach, the combined heat transfer coefficients between the glass surfaces and indoor and outdoor environments can be considered as in EN 673 [33][5], $h_{out} = 25\ \mathrm{W/(m^2K)}$, $h_{in} = 3.6 + 4.1\varepsilon/0.837\ \mathrm{W/(m^2K)}$. Note that this standard also uses the aproximated value of h^{rad} in Eq. (7) to model the radiative conductance of the gas spaces in multiple glazing, with an *a priori* value of $T_m = 283$ K.

On the modeling of the heat transfer coefficients through the natural/forced convection and thermal radiation, see *e.g.*, ISO 15099 [5] or, in the scope of PV modules, Fung and Yang [10], Skandalos and Karamanis [11] and references therein. It should be recalled that, in any case, the g-value is a function of the boundary conditions of the problem.

2.3. Solar heat gain coefficient of a layer stack

The union of n layers will be now considered, as shown by Fig. 2. Each layer has a thickness denoted as e_i, conductivity k_i ($R_i = e_i/k_i$) and integrated absorption $\bar{A}_i$, $i = 1, 2, \ldots, n$. Let T_{out}, R_{out}, T_{in} and R_{in} be the boundary conditions for temperatures and thermal resistances of the outdoor and indoor environments. In order to apply the nodal plane approach, let T_i^s and T_i be the nodal temperature of the ith layer, for the cases of solar irradiation from outside and no irradiance, respectively.

If there is no solar irradiation, $q_{i,i+1}$ is defined as the heat flux between the ith and $(i+1)$th central nodal-planes (set $q_{0,1} = q_{out}$ and $q_{n,n+1} = q_{in}$). In the steady-state situation, there is a sole heat flux, q, which, by application of the second equation in (2), can be written

[4] The simplified calculation requires an *a priori* estimation of the T_m value, in order to avoid the temperature nodes T_1 and T_2 within the heat transfer coefficients. The most straightforward consists in taking T_m as the T_{in} and T_{out} boundary values.

[5] For a non coated glass surface, $\varepsilon = 0.837$ then $h_{in} = 7.7\ \mathrm{W/(m^2K)}$. h_{in} and h_{out} values were updated in the 2011 versions of EN 673/EN 410, regarding the previous values from ISO 10292 [34].

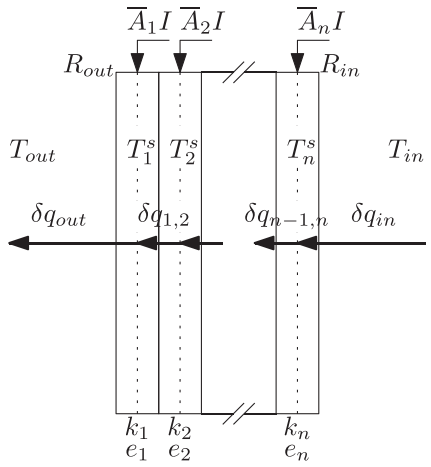

Fig. 2. Scheme of a n-layer stack.

as

$$q = q_{out} = \frac{T_1 - T_{out}}{R_{out} + \frac{1}{2}\frac{e_1}{k_1}} = q_{1,2} = \frac{T_2 - T_1}{\frac{1}{2}\frac{e_1}{k_1} + \frac{1}{2}\frac{e_2}{k_2}} = \cdots = q_{in} = \frac{T_{in} - T_n}{R_{in} + \frac{1}{2}\frac{e_n}{k_n}}. \tag{8}$$

Besides, considering the total thermal resistance of the system, $R_{tot} = R_{out} + R_1 + \cdots + R_n + R_{in}$,

$$q = \frac{T_{in} - T_{out}}{R_{tot}} \equiv U(T_{in} - T_{out}) \tag{9}$$

where the thermal transmittance (or standardized U-value), $U = 1/R_{tot}$, has been introduced for notational convenience. Note from denominators of Eq. (8), that it will be useful to define the modified thermal resistances,

$$\tilde{R}_{out} = R_{out} + \frac{1}{2}\frac{e_1}{k_1},\ \tilde{R}_{in} = R_{in} + \frac{1}{2}\frac{e_n}{k_n},\ \tilde{R}_{i,i+1} = \frac{1}{2}\frac{e_i}{k_i} + \frac{1}{2}\frac{e_{i+1}}{k_{i+1}},$$
$$i = 1, 2, \ldots, n-1, \tag{10}$$

which also verify, $R_{tot} = \tilde{R}_{out} + \tilde{R}_{12} + \cdots + \tilde{R}_{n-1,n} + \tilde{R}_{in}$.

The case of solar irradiation from the outside will be considered now. The heat flux difference from the former case, $\delta q_{i,i+1}$, will be defined analogously, so that between the ith and $(i+1)$th nodal planes the relation $q^s_{i,i+1} = q + \delta q_{i,i+1}$ holds. Given the first Eq. in (2), the following relations are fulfilled

$$\begin{cases} \delta q_{out} - \delta q_{1,2} & = I\bar{A}_1, \\ \delta q_{i,i+1} - \delta q_{i+1,i+2} & = I\bar{A}_{i+1}, \quad i = 1, 2, \ldots, n-2, \\ \delta q_{n-1,n} - \delta q_{in} & = I\bar{A}_n. \end{cases} \tag{11}$$

forming a linear system of n equations and $n+1$ unknowns (δq). The missing equation in order to provide a particular solution is obtained from the relation between the $q^s_{i,i+1}$ through the nodal temperatures, *i.e.*,

$$q^s_{i,i+1} = q + \delta q_{i,i+1} = \frac{T^s_{i+1} - T^s_i}{\tilde{R}_{i,i+1}},\ i = 0, 2, \ldots, n \tag{12}$$

with $\delta q_{0,1} = \delta q_{out}$, $\delta q^s_{n,n+1} = \delta q_{in}$, $\tilde{R}_{0,1} = \tilde{R}_{out}$, $\tilde{R}_{n,n+1} = \tilde{R}_{in}$, and $T^s_0 = T_0 = T_{out}$, $T^s_{n+1} = T_{n+1} = T_{in}$, used for notational convenience. Using Eq. (8) for q,

$$\delta q_{i,i+1} = \frac{(T^s_{i+1} - T_{i+1}) - (T^s_i - T_i)}{\tilde{R}_{i,i+1}},\ i = 0, 1, 2, \ldots, n \tag{13}$$

which can be suitably added in order to remove the unknown nodal temperatures, and obtain the following relation among fluxes and resistances,

$$\tilde{R}_{out}\delta q_{out} + \tilde{R}_{1,2}\delta q_{1,2} + \tilde{R}_{2,3}\delta q_{2,3} + \cdots + \tilde{R}_{n-1,n}\delta q_{n-1,n} + \tilde{R}_{in}\delta q_{in} = 0. \tag{14}$$

The system of equations comprising Eqs. (11) and (14) can be written in matrix form as follows:

$$\begin{pmatrix} 1 & -1 & \cdots & 0 & 0 \\ 0 & 1 & \cdots & 0 & 0 \\ \vdots & \vdots & \ddots & \vdots & \vdots \\ 0 & 0 & \cdots & 1 & -1 \\ \tilde{R}_{out} & \tilde{R}_{1,2} & \cdots & \tilde{R}_{n-1,n} & \tilde{R}_{in} \end{pmatrix} \begin{pmatrix} \delta q_{out} \\ \delta q_{1,2} \\ \vdots \\ \delta q_{n-1,n} \\ \delta q_{in} \end{pmatrix} = \begin{pmatrix} I\bar{A}_1 \\ I\bar{A}_2 \\ \vdots \\ I\bar{A}_n \\ 0 \end{pmatrix}. \tag{15}$$

For the SHGC calculation, only the δq_{in} heat flux is of interest. The system of equations can be solved by the Gauss-Jordan elimination method. The $(n+1)\times(n+1)$ matrix of the system is reduced to a triangular form by means of the following sequence of row operations: $-\tilde{R}_{out} \times F_1 + F_{n+1}$, $-(\tilde{R}_{out} + \tilde{R}_{1,2}) \times F2 + F_{n+1}$, and so on, F_i being the ith row. Then the last equation of the equivalent system results in

$$R_{tot}\delta q_{in} = -\tilde{R}_{out} I\bar{A}_1 - (\tilde{R}_{out} + \tilde{R}_{1,2}) I\bar{A}_2 - \cdots$$
$$-(\tilde{R}_{out} + \tilde{R}_{1,2} + \ldots + \tilde{R}_{in}) I\bar{A}_n \tag{16}$$

or, equivalently, by recovering the original thermal resistances

$$\delta q_{in} = -I\sum_{i=1}^{n} \bar{A}_i \frac{R_{out} + \left(\sum_{j=1}^{i-1} R_j\right)_{i>1} + R_i/2}{R_{tot}} \tag{17}$$

Note that $\delta q_{in} < 0$, implying a thermal gain of the indoor environment.

Then, the net heat flux in the situation of solar irradiation is given by

$$q^s = q + \delta q_{in} - \bar{T}I = U(T_{in} - T_{out}) - (I\bar{T} + |\delta q_{in}|), \tag{18}$$

which, considering definition (5) of the SHGC, implies

$$g = \bar{T} + |\delta q_{in}|/I = \bar{T} + \sum_{i=1}^{n} \bar{A}_i \frac{R_{out} + \left(\sum_{j=1}^{i-1} R_j\right)_{i>1} + R_i/2}{R_{tot}}. \tag{19}$$

This expression will be used in the current study to obtain the g-value of a PV module structure, comprising the encapsulation materials (mainly glass and polymeric interlayers) and solar cells. However, the expression can be used in a more general way (as it is a general algebraic relation between thermal resistances of a multilayered structure), for instance, in the case of multiple glazing (including gas chambers).

The $|\delta q_{in}|/I$ ratio is known as secondary heat transfer factor in glazing standards. The general expression for this factor given by Rosenfeld [29] for glazing systems is (Eq. (2) of the reference, written with this paper's notation) $|\delta q_{in}|/I = (R_{out} + \gamma R_s)\bar{A}/R_{tot}$, R_s and $\bar{A}$ being the thermal resistance and absorptance of the glazing, and γ the normalized average thermal resistance between the outer surface of the system and the planes where the solar radiation is absorbed. This expression is equivalent to Eq. (17) when γ parameter is obtained for a multilayered structure under the same modeling hypothesis of this work [35], $\gamma = \sum_{i=1}^{n} \bar{A}_i R_{0i}/(\bar{A}R_s)$, R_{0i} being the thermal resistance between the centre of the ith layer and the outer surface of the system. The approach of Hermanns et al. [30] for the thermal response of a single pane is also equivalent to Rosenfeld [29], by means of the relation $\gamma = 1 - \beta_e/\bar{A}$, β_e being the direct absorptance moment introduced by these authors,

related with the spatial distribution of radiation absorption within the glass pane.

3. Simplified calculation of the SHGC of a BIPV module

In this section, the former Eq. (19) for the SHGC will be applied to a conventional laminated BIPV module, consisting in front and rear encapsulation materials and a specific surface distribution of opaque PV cells. This subject is addressed in three steps: the optical modelling of the system, the effective absorptance of the encapsulated cell, considering the conversion of a portion of the incident solar energy into electricity, and the integration of these features within the thermal model previously developed.

3.1. The optical modelling

Expression (19) for the g-value includes short-wave spectrum-integrated energy magnitudes, namely, the total transmittance $\bar{T}$, and the layer absorptions $\bar{A}_i$. These parameters must be obtained from the optical modelling of the PV module. Such a problem has been previously tackled by Baenas and Machado [8] and Machado et al. [9], with a basis on the classical transfer matrix methods (see, *e.g.*, Harbecke [36], or Heavens [37] for the characteristic matrices theory background).[6] The modeling hypothesis, following the approach of the previously mentioned standards (mainly the approximation of incoherent superposition of radiation, near-normal incidence and no light diffusion), allow the formulation of closed analytical solutions for these energy magnitudes, which is essential to fulfill the purpose of this work. For consistency reasons, the analytical expressions for these energy magnitudes are equivalent to those of EN 410 [4] and ISO 9050 [3] standards, in the transparent region. However, these regulations do not address the situation of an opaque component within the optical system, which must be treated as a singular solution of the general system of equations for the energy coefficients of the glazing system (the optical components are not well defined in the case of null transmissivity). This subject has been addressed by the authors in the previously mentioned references.

The optical modelling yields the short-wave spectral energy magnitudes of the PV module (transmittance, T, reflectance, R, and absorptance, A), in terms of internal magnitudes of the system components (transmissivity, τ or t, or reflectivity, ρ or r). Note that all these parameters, depicted in Fig. 3, are spectral, although the wavelength argument is omitted for the sake of simplicity. The spectrum-integrated (or averaged) magnitudes are then calculated following the standards, using discretized spectral distributions of the incoming solar flux (ISO 9050 or EN 410 for glazing, ASTM G173-03, [42] or IEC 60904-3, [43] for PV modules,[7] etc.). These averaged parameters are symbolized with a top bar ($\bar{T}$, $\bar{R}$ and $\bar{A}$).

In Fig. 3 and the following formulae, subscripts *g* and *l* are used for glass and interlayer film, respectively. Subscript *cell* is used to refer to the opaque solar cell, and *enc* is used for the ensemble of encapsulation materials (*i.e.*, glass and interlayer). On the other hand, superscripts *st* and *op* are used to denote the transparent and opaque regions of the module, and *f* and *b* are used for front and back directions.

It should be taken into account that all the previous spectral magnitudes can be experimentally obtained by UV–vis–NIR spectrophotometry at near-normal incidence, by means of specific basic configurations allowing the separate characterization of each component, following EN 410 [4], Rubin et al. [39] or Baenas and Machado [44,8], among others. For the sake of completeness, the expressions of the absorptances needed for the further development of this work are listed below. They are calculated from the basic set of optical parameters r_{g1}, r_{g2}, τ_{g1}, τ_{g2} and τ_l and have been extracted, except for notation, from Baenas and Machado [8].

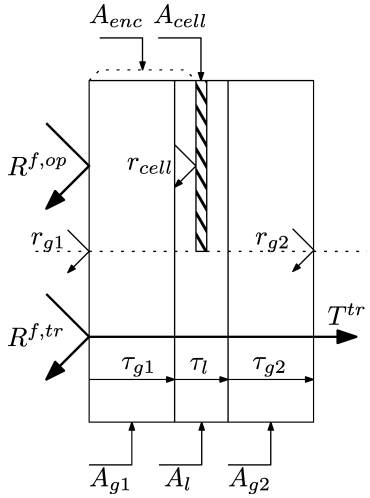

Fig. 3. Scheme of the optical model for a BIPV module.

In the opaque region, the expressions

$$\begin{aligned} r_{cell} &= \frac{R^{f,op} - r_{g1}}{\tau_{g1}^2 \tau_l^2 (1 - 2r_{g1} + R^{f,op} r_{g1})}, \\ A_{enc} &= (1 - r_{g1})(1 - \tau_{g1}\tau_l) \frac{1 + \tau_{g1}\tau_l r_{cell}}{1 - r_{g1} r_{cell} \tau_{g1}^2 \tau_l^2}, \\ A_{cell} &= (1 - r_{g1})(1 - r_{cell}) \frac{\tau_{g1}\tau_l}{1 - r_{g1} r_{cell} \tau_{g1}^2 \tau_l^2}, \end{aligned} \tag{20}$$

are fulfilled, and there is no transmission or short-wave absorption on the rear glass. In the transparent region,

$$\begin{aligned} A_{g1} &= (1 - r_{g1})(1 - \tau_{g1}) \frac{1 + \tau_{g1}\tau_{g2}^2\tau_l^2 r_{g2}}{1 - r_{g1} r_{g2} \tau_{g1}^2 \tau_{g2}^2 \tau_l^2}, \\ A_l &= (1 - r_{g1})(1 - \tau_l)\tau_{g1} \frac{1 + r_{g2}\tau_l\tau_{g2}^2}{1 - r_{g1} r_{g2} \tau_{g1}^2 \tau_{g2}^2 \tau_l^2}, \\ A_{g2} &= (1 - r_{g1})(1 - \tau_{g2})\tau_{g1}\tau_l \frac{1 + r_{g2}\tau_{g2}}{1 - r_{g1} r_{g2} \tau_{g1}^2 \tau_{g2}^2 \tau_l^2}, \end{aligned} \tag{21}$$

while the transmittance T^{tr} can be obtained, for instance, following EN 410 [4], or equivalently,

$$T^{tr} = (1 - r_{g1})(1 - r_{g2}) \frac{\tau_{g1}\tau_l\tau_{g2}}{1 - r_{g1} r_{g2} \tau_{g1}^2 \tau_{g2}^2 \tau_l^2}. \tag{22}$$

In a standard PV cell, with $r_{cell} \ll 1$ (mainly due to the presence of antireflective – AR – coatings in the interlayer-cell interface, for the usual values of the refractive indices of the laminate components), the non-normal incidence case can be tackled in good numerical approximation by substituting in the previous expressions the internal transmissivities τ by $\tau^{1/\cos\theta_r}$, θ_r being the irradiation angle of refraction, and calculating $r_g(\theta)$ according to Fresnel equations, θ being the irradiation angle of incidence ($\theta = 0$ for normal incidence) [45]. By application of the considered optical model, rigorous expressions for other types of multilayered structures can be achieved, for instance, including AR coatings in the outdoor-front glass interface, low-emissivity coatings in the indoor-rear glass, or even embedded coatings if necessary.

[6] Other approaches can be followed, as for instance those based on the classical ray-tracing methods. See, *e.g.*, Furler [38] and Rubin et al. [39] or, within the PV modules scope, Krauter and Hanitsch [40] and Lu and Yao [41], among others.

[7] Both standards provide an AM1.5 global distribution spectrum corresponding to an integrated irradiance of 1000 W/m^2 incident on a sun-facing plane surface tilted at 37° to the horizontal, IEC 60904-3 being a more recent update.

3.2. The effective absorptance of the PV cell

Under working conditions of a PV module, a portion of the incident solar energy is converted into electricity, and taken out of the system. In a first approximation, this mechanism can be described by means of spectrum-averaged magnitudes,[8] such as the PV module conversion efficiency, $0 \leq \eta < 1$, a dimensionless magnitude defined as $\eta = P_{el}/I$, P_{el} being the electrical (DC) PV generation power (per unit area). Then, for the purpose of calculating the SHGC of a PV module, the previous absorptance $\bar{A}_{cell}$ will be substituted by an effective one, $\bar{A}^{eff}_{cell}$, which takes into account the loss of energy due to PV generation.

It can be assumed that the internal efficiency of the cell (*i.e.*, the relation between absorbed and generated powers, inside the PV cell), will not vary among the bare and encapsulated situations (Koo et al. [46]), except for the inherent temperature dependence (see, *e.g.*, Skoplaki and Palyvos [47]). Therefore, if P^{bare}_{el} and P^{ec}_{el} are the PV generated electrical powers of the bare and encapsulated solar cell, respectively, the relation $P^{bare}_{el}/I = P^{ec}_{el}/(\bar{\phi} I)$ will be fulfilled, $\bar{\phi}$ being the integrated factor of the solar flux incident on the encapsulated cell, *i.e.*, inside the module. Correspondingly, $\eta_{ec} = \bar{\phi}\eta_{bare}$. Note that the integrated effective absorptance of the encapsulated solar cell will be hence given by

$$\bar{A}^{eff}_{cell} = \bar{A}_{cell} - \eta_{ec}. \tag{23}$$

Although it is assumed that the PV cells in a module display a very similar electrical performance in ideal conditions (*e.g.*, no shadowing), strictly speaking the efficiency of the least producing cell should be used in the calculation, taking a conservative approach.

The $\bar{\phi}$ parameter can be determined by means of the optical model referred in the previous section. Specifically, following Baenas and Machado [8], the spectral factor of solar flux incident on the encapsulated cell, ϕ, is given by the back radiosity of the encapsulation materials (J_{1b}, in the layer-by-layer absorption calculation),

$$\phi = (1 - r_{g1})\frac{\tau_{g1}\tau_l}{1 - r_{g1}r_{cell}\tau^2_{g1}\tau^2_l} = \frac{A_{cell}}{1 - r_{cell}} \tag{24}$$

where the second equality comes from the comparison with the third equation in (20). Subsequently, $\bar{\phi}$ is the related solar spectrum-integrated magnitude. Let $S(\lambda)$ be the normalized relative spectral distribution of the solar radiation, and $[\lambda_1, \lambda_2]$ the relevant wavelength range (both depending on the particular standard considered). Then, Eq. (24) leads to,

$$\eta_{ec} = \eta_{bare}\int_{\lambda_1}^{\lambda_2} S(\lambda)\frac{A_{cell}(\lambda)}{1 - r_{cell}(\lambda)}d\lambda, \tag{25}$$

allowing a direct calculation of $\bar{A}^{eff}_{cell}$ from η_{bare}, which is a common design parameter provided by solar cell manufacturers.

As stated above, for usual PV cells, $r_{cell} \ll 1$, enabling the approximation $\phi \simeq A_{cell}$, and therefore $\eta_{ec} \simeq \bar{A}_{cell}\eta_{bare}$. In such a situation, the integrated effective absorptance of the solar cell is given by,

$$\bar{A}^{eff}_{cell} = \bar{A}_{cell} - \eta_{ec} \simeq \bar{A}_{cell}(1 - \eta_{bare}). \tag{26}$$

This is a practical (but approximate) relation, simplifying the calculation of this portion of the SHGC.

It is known that solar cells performance significantly decreases with operating temperature increase. A comprehensive compilation of the correlations between this temperature and the weather variables and boundary conditions can be found in Skoplaki and Palyvos [47]. The traditional one is the linear relation (Evans and Florschuetz [48])

$$\eta(T) = \eta_{T_{ref}}[1 - \beta_{ref}(T - T_{ref})], \tag{27}$$

T_{ref}, $\eta_{T_{ref}}$ and β_{ref}, being reference parameters for temperature, electrical efficiency and linear temperature coefficient (at reference temperature), defined under a specific solar irradiance.[9]

Besides solar irradiance absorption, the operating temperature of the module depends on Joule (heating) effect, related to the heat released by the passage of the electrical current through resistive conductors. The associate temperature variation has been quantified by numerical experimentation based on multiphysics finite element (FE) modelling of the PV module, for instance, by Acciani et al. [49] or Nyanor et al. [50]. It has been proved that Joule effect has a minimal influence on the overall PV module temperature (less than 5%) when the calculation is performed in normal operating cell temperature (NOCT). This fact, together with the complexity associated to the modeling of the Joule effect from the design parameters of the PV module, justifies the neglection of its influence on the effective absorptance of the solar cell.

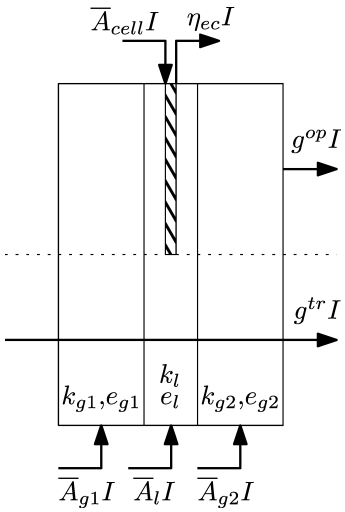

Fig. 4. Scheme of the BIPV module thermal model.

3.3. The solar heat gain coefficient of a BIPV module

From the consideration of the previous sections, a closed-analytical expression for the SHGC of a three-layer standard BIPV module, depicted in Figs. 3 and 4, can be given.

The *g*-value is divided in two parts, corresponding to the opaque, g^{op}, and transparent, g^{tr}, regions. If f is the ratio of transparent to total area, the total SHGC will be given, in a first approximation, by the linear relation,[10]

$$g = (1 - f)g^{op} + fg^{tr}. \tag{28}$$

[8] PV conversion is more accurately characterized by means of the External Quantum Efficiency (EQE) spectral function, defined as the ratio of charge carriers collected by the solar cell to the number of photons incident on the cell, at a given wavelength. A calculation in terms of this magnitude, however, requires a more complex experimental characterization of the PV cell [8].

[9] Usual design values are, *e.g.*, $T_{ref} = 25\,^{\circ}C$, $\eta_{T_{ref}} = 0.15$, $\beta_{ref} = 0.0041\,^{\circ}C^{-1}$, $I_{ref} = 1000\,W/m^2$, for a c-Si PV cell (Skoplaki and Palyvos [47], and references therein). It should be noted that these values depend on the solar cell technology and that a wide range of commercial solar cells (including thin film or other technologies) is currently available for BIPV applications. Usually, $\eta_{T_{ref}}$ and β_{ref} are given by the PV manufacturer for the bare cell.

[10] Any type of thermal edge effects are neglected in such a relation. However, some experimental measurements of the *g*-value of a PV module have confirmed that the linear correlation with the surface ratio f can be assumed (see, *e.g.*, Olivieri et al. [24]).

Therefore, by using Eq. (19), $g^{op} = \left|\delta q_{in}^{op}\right| / I$ and $g^{op} = \bar{T}^{tr} + \left|\delta q_{in}^{tr}\right| / I$, so that the following expressions are obtained,

$$\begin{aligned} g^{op} = & \frac{\bar{A}_{enc}}{R_{tot}}\left(R_{out} + \frac{1}{2}\frac{e_{enc}}{k_{enc}}\right) + \frac{\bar{A}_{cell}^{eff}}{R_{tot}}\left(R_{out} + \frac{e_{enc}}{k_{enc}} + \frac{1}{2}\frac{e_{cell}}{k_{cell}}\right), \\ g^{tr} = & \bar{T}^{tr} + \frac{\bar{A}_{g1}}{R_{tot}}\left(R_{out} + \frac{1}{2}\frac{e_{g1}}{k_{g1}}\right) + \frac{\bar{A}_{l}}{R_{tot}}\left(R_{out} + \frac{e_{g1}}{k_{g1}} + \frac{1}{2}\frac{e_{l}}{k_{l}}\right) \\ & + \frac{\bar{A}_{g2}}{R_{tot}}\left(R_{out} + \frac{e_{g1}}{k_{g1}} + \frac{e_{l}}{k_{l}} + \frac{1}{2}\frac{e_{g2}}{k_{g2}}\right), \end{aligned} \tag{29}$$

where the equations of the optical modelling, (20) and (21), and the effective absorption of the solar cell given by Eq. (23), must be considered. Note that, for the sake of simplicity, the equivalent thermal conductivity k_{enc}, defined by means of $e_{enc}/k_{enc} = e_{g1}/k_{g1} + e'_l/k_l$, e'_l being the thickness of interlayer in the solar cell area and $e_{enc} = e_{g1} + e'_l$, has been used for the encapsulation materials within the opaque region.

For nominal (standardized) and usual design values of thickness and thermal conductivity of glass ($k_g \sim 1$ W/mK, $e_g \sim 4\times10^{-3}$ m) and polymeric interlayers ($k_l \sim 0.20$ W/mK, $e_l \sim 4\times10^{-4}$ m), the approximation $e/k \ll R_{out}$ can be considered, allowing simpler expressions for the g-value,

$$g^{op} \simeq \frac{R_{out}}{R_{tot}}\left(\bar{A}_{enc} + \bar{A}_{cell}^{eff}\right), \quad g^{tr} \simeq \bar{T}^{tr} + \frac{R_{out}}{R_{tot}}(\bar{A}_{g1} + \bar{A}_{l} + \bar{A}_{g2}). \tag{30}$$

Strictly, the approximate g^{tr}-value of the EN 410 [4] and ISO 9050 [3] standards is obtained by expressing Eq. (30) in terms of the heat transfer coefficients. For instance, the standardized g-value of a simple glazing (one layer) results in

$$g^{tr} \simeq \bar{T} + \frac{R_{out}}{R_{tot}}\bar{A} = \bar{T} + \frac{h_{in}}{h_{out} + h_{in}}\bar{A}. \tag{31}$$

The validity of the standardized expression of the g^{tr}-value is also discussed in Rosenfeld et al. [35] and in Hermanns et al. [30]. In a similar way, the expressions given by standards for double and triple glazing can be recovered from g^{tr} in Eq. (29) by introducing the expression of the thermal resistance of the gas chambers, $R_g = h_g^{-1} = (h_g^{rad} + h_g^{conv})^{-1}$, following the same normative texts for the modelling of the combined heat transfer coefficients.

The approximate expression is better for g^{tr} than for g^{op}. This is due to the fact that $\bar{T}$ is by far the main contribution to g^{tr} in the case of semitransparent PV structures with high solar transmittance. The approximate total g-value reaches the second significant figure for the usual design values of a standard PV module, as will be shown in the next section. This numerical simplification gets worse for multilayered PV modules of polymeric materials (polycarbonate, ETFE, etc.), with low thermal conductivities.

4. A real case of study

In this section, the formerly derived expressions will be applied to a particular case and compared with experimental measurements and numerical calculations found in the specific literature. In this way, the simplified calculation of the SHGC will be performed emulating the design phase of a PV element.

The experimental data and numerical model for the estimation of the solar factor of BIPV modules carried out by Mazzali et al. [21] have been considered of interest. These authors perform the SHGC experimental characterization by means of a calorimeter equipped with a solar simulator, set to reproduce the ISO 9050 [3] standardized value of the heat transfer coefficients, $h_e = 23 \pm 3$ W/(m^{2}K) and $h_i = 8 \pm 1$ W/(m^{2}K) (for an indoor surface hemispherical emissivity of 0.837), and a UV/vis/NIR spectrophotometer for the optical measurements of the samples.

Table 1
Comparison of SHGC values as a function of the operating modes.

Test	g_{exp}	g_{num}	g_{cal} (this work)
OC	0.45 ± 0.04	0.45	0.45
MPP	0.43 ± 0.04	0.43	0.43

Table 2
Effect of operating temperature in SHGC and Δg values.

Test	g_{exp}	Δg_{exp}	g_{cal}	Δg_{cal}
OC	0.45 ± 0.04		0.4527	
MPP, $\eta_{ec}(25\,^\circ C) = 0.1371$	0.43 ± 0.04	4.44%	0.4295	5.13%
MPP, $\eta_{ec}(45\,^\circ C) = 0.1262$			0.4313	4.72%

A comprehensive explanation of the numerical method proposed by Mazzali et al. [21] can also be found in Zinzi et al. [51] and Scarpa et al. [52]. It is based on a finite difference model in order to obtain the temperature nodes in a set of ISO 15099-like heat balance equations, by means of an iterative procedure.

The structure of the laminated BIPV specimen is that of a glass–glass PV module, with a 4 mm thickness extra-clear (low-iron) glass and 0.38 mm of PVB (polyvinyl butyral) interlayer as superstrate, polycrystalline silicon cells (in the opaque region), and 0.38 mm of PVB and 4 mm of float clear glass in the substrate. The opaque region contains 25 square cells of 156×156 mm^2 in a sample size of 995×995 mm^2, giving a transparent to opaque surface ratio $f = 0.385 \simeq 40\%$. The nominal electrical conversion efficiency of bare cells is $\eta_{bare} = 0.15$.

In order to perform the analytical calculation, the optical characterization of analogous elements has been reproduced for this work, using a UV/vis/NIR spectrophotometer (JASCO V-670) equipped with a 150 mm integrating sphere, calibrated in the 300–2200 nm wavelength range. Fig. 5 shows some relevant curves of the performed optical characterization. By means of Eqs. (20) and (21), the following averaged magnitudes were found: $\bar{A}_{enc} = 0.0471$ and $\bar{A}_{cell} = 0.8635$ in the opaque region; $\bar{A}_{g1} = 0.0214$, $\bar{A}_{l} = 0.0401$, $\bar{A}_{g2} = 0.1520$ and $\bar{T}^{st} = 0.7152$ in the transparent zone. All the integrated parameters have been computed with the ASTM G173-03 [42] discretized spectral distribution, commonly used in photovoltaic applications. Through Eq. (25), $\eta_{ec} = 0.1371$ is obtained for the efficiency of the solar cell in encapsulated configuration. The design parameters of the components are given by the standards and manufacturers, $k_{g1} = k_{g2} = 1$ W/mK, $k_l = 0.20$ W/mK, $e_{g1} = e_{g2} = 4$ mm, $e_l = 0.38$ mm (per film). There is one interlayer film in the opaque region, and two in the transparent one.

Therefore, by applying Eq. (29) the analytical g-values (g_{cal}) obtained will be compared with the experimental and numerical values of the SHGC (g_{exp} and g_{num}) from Mazzali et al. [21] (Table 4 of the reference), in two operating conditions: *open circuit* (OC) – without an electric load, *i.e.*, with $\eta_{ec} = 0$; and at *maximum power point* (MPP) – at the point of maximum power generation – with the previously estimated values of η_{ec} parameter. The results of this comparison are collected in Table 1.

Note that in the OC and MPP situation, the theoretical SHGC values (numerical and closed-analytical) match the central value within the experimental uncertainty ranges, up to the second significant figure of the g-value, which is the usual accuracy requirement.

If the approximate Eq. (30) are used instead of Eq. (29), the following values are obtained: $g_{cal} = 0.44$ (OC), $g_{cal} = 0.42$ (MPP). Note that the second significant figure is affected.

In Table 2, SHGC values with a higher accuracy are displayed. Two situations have been considered: in the first one, the former

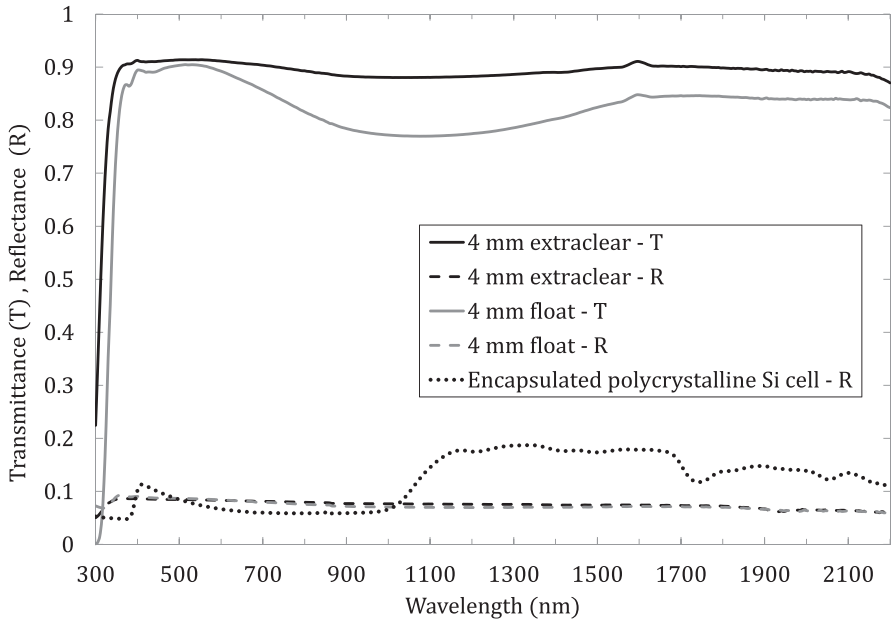

Fig. 5. Spectrophotometric curves of the optical characterization of the BIPV module (this work).

η_{ec} = 0.1371 value of the conversion efficiency is used. In the second one, the conversion efficiency is corrected by using Eq. (27), considering an estimated module operating temperature of 45 °C (see, *e.g.*, FSEC standard [53]), which gives η_{ec} = 0.1262. Δg represents the relative variation (%) of the *g*-value between the OC and MPP conditions.

Table 2 shows that, although in this case the *g*-value rounded up to two significant figures is not sensitive to slight variations of the electrical power conversion efficiency of the cell, by comparing the Δg_{cal} values with nominal (experimental) ones, it is convenient to correct the efficiency value with an estimation – or design value – of the operating temperature of the cell (Skoplaki and Palyvos [47]). In this case, there is a good agreement between the theoretical prediction Δg_{cal} = 4.72% and the experimental value, Δg_{exp} = 4.44%, which is directly related with the modeling of the effective absorptance of the solar cell.

All the Δg values are consistent with the experimental study of Chen et al. [22], in which it is concluded that, when electric loads are present, the SHGC of semitransparent BIPV modules is reduced from 3 to 6%, proportionally to the electric power output.

5. Conclusions

In this paper, a closed-analytical expression for the SHGC of a glass–glass BIPV module has been constructed *ab initio*, for the case of normal incidence of the solar radiation. This expression is useful to perform simplified calculations by decoupling the convective-conductive and radiative parts of the heat transfer problem from the temperature nodes. The use of more complex iterative procedures to solve the non-linear equations of the thermal balance can be therefore avoided. The analytical formula allows the use of standardized or design values for the involved physical parameters. This approach is in line with the most widely used glazing standards and, consequently, with the recent EN 50583 standard for BIPV modules and systems. The usual requirement from the glazing, façades and BIPV sectors, *i.e.*, the *a priori* calculation of the SHGC, can be also fulfilled with the proposed approach. Additionally, in the transparent region of the BIPV module, the equivalence between the derived expression of the *g*-value and other existing thermal models has been established, including those of the EN 410/ISO 9050 standards. In order to overcome the limitations posed by the use of standardized boundary conditions, the proposed model can also be applied to the case of non-standardized boundary conditions through the classical approach of linear treatment of the combined convection–radiation heat transfer equations, as discussed in Section 2.2, or the use of iterative procedures for the non-linear situation.

It has been shown that this analytical calculation of the SHGC is in excellent agreement with a real case of study, which includes external experimental data and numerical determinations of the solar factor. The theoretical prediction of the variation of the SHGC between the open circuit and maximum power point operating modes also shows very good agreement with experiments. This simplified method shows a clear operational advantage with respect to numerical procedures. Additionally, the outlined approach can be extended to more complex configurations of BIPV modules.

As previously described, the optical characterization of the module components required by the method is analogous to the one required by glazing standards. It can even be reduced to the characterization of basic configurations in order to obtain the spectral reflectivity of the encapsulation–cell interface, given that the parameters for other module architectures can be obtained from calculations. The experimental work can be also minimized from the use of public databases (*e.g.*, the international Glazing Database – IGDB[11] – maintained and published by Lawrence Berkeley National Laboratory), which provide spectral transmittance and reflectance data of encapsulation materials (simple and laminated glass, from which the transmissivity of the interlayer can be obtained). The thermal parameters and cell efficiency can be taken from standardized or design values, generally provided by the manufacturers. The experimental characterization of the above properties is therefore less time intensive and costly than the g-value measurement based on calorimetric methods.

[11] http://windowoptics.lbl.gov/data/igdb/igdb.

As a further application, this work can be considered a proposal for completion and compliance with the requirements of the new EN 50583 BIPV standard, which, in its "Energy economy requirements" section states that "In addition to the procedures defined in EN 410 to determine the total solar energy transmittance (*g*-value) of glazing materials, calculations or measurements are permitted that take the removal of energy from the system as electricity into account". This normative text stems the thermal and related optical modeling of the BIPV module to glazing standards EN 410 and EN 673. However these standards do not include the needed calculation of the short-wave absorptances of each separate component of the system, and, in particular, the effective absorptance of the solar cell, which is related with its electrical power conversion efficiency, in encapsulation conditions. Besides, the expression of the SHGC given by the standards is an approximate case that can affect the second significant figure of the *g*-value as it has been demonstrated. All these features are indeed addressed in the analytical model presented herein.

Acknowledgements

This work has received funding by the European Union's Horizon 2020 research and innovation programme under Grant Agreement No. 691768. This document reflects only the authors' views and not those of the European Commission. The Commission is not responsible for any use that can be made of the information contained herein.

References

[1] Directive 2010/31/EU of the European Parliament and of the Council of 19 May 2010 on the energy performance of buildings, Off. J. Eur. Union L153 (2010) 13–35.
[2] Directive 2012/27/EU of the European Parliament and of the Council of 25 October 2012 on energy efficiency, Off. J. Eur. Union L315 (2012) 1–56.
[3] ISO 9050 (International Standard), Determination of Light Transmittance, Solar Direct Transmittance, Total Solar Energy Transmittance, Ultraviolet Transmittance and Related Glazing Factors, 2003.
[4] EN 410 (European Standard), Glass in Buildings. Determination of Luminous and Solar Characteristics of Glazing, 2011.
[5] ISO 15099 (International Standard), Thermal Performance of Windows, Doors and Shading Devices. Detailed Calculations, 2003.
[6] EN 13363-2 (European Standard), Solar Protection Devices Combined with Glazing – Calculation of Total Solar Energy Transmittance and Light Transmittance – Part 2: Detailed Calculation Method, 2005.
[7] EN50583-1,2 (European Standard), Photovoltaics in Buildings – Part 1: BIPV Modules – Part 2: BIPV Systems, 2016.
[8] T. Baenas, M. Machado, Optical model for multilayer glazing systems: application to laminated glass and photovoltaic modules, Solar Energy 125 (2016) 256–266.
[9] M. Machado, T. Baenas, N. Yurrita, Optical model for multilayer glazing systems: experimental validation through the analytical prediction of encapsulation-induced variation of PV modules efficiency, Solar Energy 135 (2016) 77–83.
[10] T.Y.Y. Fung, H. Yang, Study on the thermal performance of semi-transparent building-integrated photovoltaic glazings, Energy Build. 40 (2008) 341–350.
[11] N. Skandalos, D. Karamanis, Investigation of thermal performance of semi-transparent PV technologies, Energy Build. 124 (2016) 19–34.
[12] K. Vats, G.N. Tiwari, Performance evaluation of a building integrated semitransparent photovoltaic thermal system for roof and façade, Energy Build. 45 (2012) 211–218.
[13] D. Infield, L. Mei, U. Eicker, Thermal performance estimation for ventilated PV facades, Solar Energy 76 (2004) 93–98.
[14] D. Infield, U. Eicker, V. Fux, L. Mei, J. Schumacher, A simplified approach to thermal performance calculation for building integrated mechanically ventilated PV facades, Build. Environ. 41 (2006) 893–901.
[15] P.W. Wong, Y. Shimoda, M. Nonaka, M. Inoue, M. Mizuno, Semi-transparent PV: thermal performance, power generation, daylight modelling and energy saving potential in a residential application, Renew. Energy 33 (2008) 1024–1036.
[16] Y. Wang, W. Tian, J. Ren, L. Zhu, Q. Wang, Influence of a building's integrated-photovoltaics on heating and cooling loads, Appl. Energy 83 (2006) 989–1003.
[17] J. Han, L. Lu, H. Yang, Thermal behavior of a novel type see-through glazing system with integrated PV cells, Build. Environ. 44 (2009) 2129–2136.
[18] T.T. Chow, Z. Lin, W. He, A.L.S. Chan, K.F. Fang, Use of ventilated solar screen window in warm climate, Appl. Therm. Eng. 26 (2006) 1910–1918.
[19] L. Liao, Numerical and Experimental Investigation of Building-Integrated Photovoltaic-Thermal Systems, 2005, Ph.D. Thesis.
[20] A. Guardo, M. Coussirat, E. Egusquiza, P. Alvedra, R. Castilla, A CFD approach to evaluate the influence of construction and operation parameters on the performance of Active Transparent Facades in Mediterranean climates, Energy Build. 41 (2009) 534–542.
[21] U. Mazzali, P. Ruggeri, M. Zinzi, F. Peron, P. Romagnoni, A. Daneo, Set-up and calibration by experimental data of a numerical model for the estimation of solar factor and U_g-value of building integrated photovoltaic systems, Energy Proc. 78 (2015) 2202–2207.
[22] F. Chen, S.K. Wittkopf, P. Khai, H. Du, Solar heat gain coefficient measurement of semi-transparent photovoltaic modules with indoor calorimetric hot box and solar simulator, Energy Build. 53 (2012) 74–84.
[23] D. Pahud, P. Gallinelli, D. Crivellin, S. Margot, R. Camponovo, M. Belliardi, G-box. Mesure in situ des performancesénergé tiques de façades transparentes et translucides. Final Report 27th June 2013, Office fédéral de l'énergie, 2013.
[24] L. Olvieri, F. Frontini, C. Polo-López, D. Pahud, E. Caamaño-Martín, G-value indoor characterization of semi-transparent photovoltaic elements for building integration: new equipment and methodology, Energy Build. 101 (2015) 84–94.
[25] T.E. Kuhn, Calorimetric determination of the solar heat gain coefficient *g* with steady-state laboratory measurements, Energy Build. 84 (2014) 388–402.
[26] F.J. Moralejo-Vázquez, N. Martín-Chivelet, L. Olivieri, E. Caamaño-Martín, Luminous and solar characterization of PV modules for building integration, Energy Build. 103 (2015) 326–337.
[27] S. Misara, Thermal Impacts on Building Integrated Photovoltaic (BIPV) (Electrical, Thermal and Mechanical Characteristics), 2014, Ph.D. Thesis.
[28] X. Shen, Energy Evaluation and Optimal Design of Semi-Transparent Photovoltaic Façade for Office Buildings in Central China, 2014, Ph.D. Thesis.
[29] J.L.J. Rosenfeld, On the calculation of the total solar energy transmittance of complex glazings, in: Proc. of 8th International meeting on Transparent Insulation Material, Freiburg, Germany, 1996.
[30] M. Hermanns, F. Ama, J.A. Hernández, Analytical solution to the one-dimensional non-uniform absorption of solar radiation in uncoated and coated single glass panes, Energy Build. 47 (2012) 561–571.
[31] J. Aguilar, Curso de termodinámica, Ed. Alhambra Longman S.A, 1989.
[32] M. Rubin, D. Arasteh, J. Hartmann, A correlation between normal and hemispherical emissivity of low-emissivity coatings on glass, Int. Commun. Heat Mass Transf. 14 (1987) 561–565.
[33] EN 673 (European Standard), Glass in Buildings. Determination of the Thermal Transmittance (, 2011.
[34] ISO 10292 (International Standard), Glass in Buildings. Calculation of Steady-State, 1994.
[35] J.L.J. Rosenfeld, W.J. Platzer, H. Van Dijk, A. Maccari, Modelling the optical and thermal properties of complex glazing: overview of recent developments, Solar Energy 69 (1–6) (2000) 1–13.
[36] B. Harbecke, Coherent and incoherent reflection and transmission of multilayer structures, Appl. Phys. 39 (3) (1986) 165–170.
[37] O.S. Heavens, Optical properties of thin films, Rep. Progr. Phys. 23 (1960) 66–69.
[38] R.A. Furler, Angular dependence of optical properties of homogeneous glasses, ASHRAE Trans. 97 (2) (1991).
[39] M. Rubin, K.V. Rottkay, R. Powles, Window optics, Solar Energy 62 (3) (1998) 149–161.
[40] S. Krauter, R. Hanitsch, Actual optical and thermal performance of PV-modules, Solar Energy Mater. Solar Cells 41/42 (1996) 557–574.
[41] Z.H. Lu, Q. Yao, Energy analysis of silicon solar cell modules based on an optical model for arbitrary layers, Solar Energy 81 (2007) 636–647.
[42] ASTM G173-03 (International Standard), Standard Tables of Reference Solar Spectral Irradiances: Direct Normal and Hemispherical on 37° Tilted Surface, 2012.
[43] IEC 60904-3 (International Standard), Photovoltaic Devices – Part 3: Measurement Principles for Terrestrial Photovoltaic (PV) Solar Devices with Reference Spectral Irradiance Data, 2016.
[44] T. Baenas, M. Machado, Optical simulation of laminated glass., in: Proc. Glass Performance Days 2009, Ed. GPD-Glaston Finland Oy, 2009, pp. 742–745.
[45] E.A. Sjerps-Koomen, E.A. Alsema, W.C. Turkenburg, A simple model of PV module reflection losses under field conditions, Solar Energy 57 (6) (1996) 421–432.
[46] Y.S. Koo, T.M. Walsh, F. Lu, A.G. Aberle, Method for quantifying optical parasitic absorptance loss of glass and encapsulant materials of silicon wafer based photovoltaic modules, Solar Energy Mater. Solar Cells 102 (2012) 153–158.
[47] E. Skoplaki, J.A. Palyvos, On the temperature dependence of photovoltaic module electrical performance: a review of efficiency/power correlations, Solar Energy 83 (2009) 614–624.
[48] D.L. Evans, L.W. Florschuetz, Cost studies on terrestial photovoltaic power systems with sunlight concentration, Solar Energy 19 (1977) 255–262.
[49] G. Acciani, O. Falcone, S. Vergura, Analysis of the thermal heating of poly-Si and a-Si photovoltaic cell by means of FEM, in: Proc. of International Conference on Renewable Energies and Power Quality, Granada, Spain, 2010.

[50] P. Nyanor, E.K. Oman, S. Kudadze, A. Deku, 3D finite element method modeling and simulation of the temperature of crystalline photovoltaic module, Int. J. Res. Eng. Technol. 4 (9) (2015) 378–384.
[51] M. Zinzi, A. Daneo, U. Mazzali, P. Ruggeri, F. Peron, Studio del comportamento radiativo e termico di componenti di involucro produttori di energia. Report Ricerca di Sistema Elettrico, ENEA Report RdS/PAR2013/, 2014140.
[52] M. Scarpa, U. Mazzali, F. Peron, Modeling the energy performance of living walls: Validation against field measurements in temperate climate, Energy Build. 79 (2014) 155–163.
[53] FSEC Standard 202-10, Test Method for Photovoltaic Module Power Rating, 2010.